Radiology Case Reports 15 (2020) 353–361

Available online at www.sciencedirect.com

ScienceDirect

journal homepage: www.elsevier.com/locate/radcr

Case Report

A large bi-lobed classic renal angiomyolipoma with vena caval extension

Nassib F. Abou Heidar, MD[a,1], *Jad A. Degheili, MD*[a,1,*], *Raja B. Khauli, MD, FACS*[a], *George Abi Saad, MD, FACS*[b]

[a] *Division of Urology, Department of Surgery, American University of Beirut-Medical Center, Riad El-Solh 1107 2020, Beirut, Lebanon*

[b] *Division of General Surgery, Department of Surgery, American University of Beirut-Medical Center, Riad El-Solh 1107 2020, Beirut, Lebanon*

ARTICLE INFO

Article history:
Received 1 December 2019
Revised 31 December 2019
Accepted 7 January 2020

Keywords:
Angiomyolipoma
Renal
Tuberous sclerosis complex
Fat emboli
Surgery
Liver mobilization

ABSTRACT

Renal angiomyolipomas (AMLs) are the most common benign renal tumors encountered, and composed of 3 components: mature adipose tissues, smooth muscles, and blood vessels. Mostly asymptomatic and discovered incidentally, the classic type of AMLs rarely extend to involve great vessels. Radiological confirmation of such lesions is paramount for diagnosis and planned intervention. Management of AMLs is based on clinical presentation and varies from active surveillance to invasive surgical interventions. A case of sizeable classic AML with extension to inferior vena cava is presented here, with successful tumor resection performed after complete liver mobilization. A literature review and a summary of similar cases are also presented. A multidisciplinary approach is required for proper and precise radiological diagnosis to achieve an adequate surgical resection, which might sometimes be complicated and complex, as in this current case.

Introduction

Angiomyolipoma (AML) is the most common mesenchymal tumors of the kidney and is mostly a benign disease [1]. This entity, first reported in 1900, Fisher described its histopathologic characteristics, in the year 1911, encompassing 3 components: mature adipose tissues, dysmorphic blood vessels, and smooth muscle fibers [2]. AML is characterized into 2 main subtypes: the classical subtype, which is almost always benign, and the epithelioid variant, which tends to behave more aggressively [3]. AML can be multicentric or solitary; they are frequently associated with tuberous

Competing Interest: The authors declare that they have no competing interests. The authors report no sources of funding in relation to this manuscript.

Acknowledgment: The authors thank Dr Ayman Tawil, Professor of clinical specialty from the Department of Pathology and Laboratory Medicine, for providing the gross and the histopathologic images with their valuable description.

* Corresponding author.
E-mail address: jdegheili@gmail.com (J.A. Degheili).

[1] Degheili and Abou Heidar contributed equally to this manuscript and both qualify as first author.

https://doi.org/10.1016/j.radcr.2020.01.005

Fig. 1 – (A) Enhanced computed tomography (CT) scan of the abdomen and pelvis with intravenous contrast, axial view, revealing a large renal mass composed solely of fat arising from the interpolar region of the right kidney (arrow), constituting an angiomyolipoma (AML). The mass measured around 13 x 19 cm. Noted as well in this axial cross-section is the bifurcation of the right renal artery (arrowhead), with 2 branches, one supplying the anterior portion and the other, the posterior portion of the right kidney. (B) Another axial cross-section of the enhanced CT scan, showing the extension of the right renal AML; cephalad abutting the liver bed, with presence of tumor fat thrombus within the infrahepatic inferior vena cava (arrow). Also noted is a small aneurysm (arrowhead) within the AML. (C) Another axial cross-section showing the extension of the renal AML with deviation of the great vessels medially, along with the presence of a minute left renal angiomyolipoma, posteriorly (arrow), measuring around 5 mm.

sclerosis or lymphangioleiomatosis and more commonly found in middle-aged females. They are usually asymptomatic but may present with gross hematuria or flank pain [4].

It is uncommon for an AML to invade into the renal vessels and extend up to the inferior vena cava (IVC), given its benign nature, especially if it is of the classic subtype. We hereby present a case of an incidental finding of a large classic AML that has extended into the renal vein, to the infrahepatic IVC, requiring a radical nephrectomy with caval thrombectomy, after complete liver mobilization.

Case presentation

A 40-year-old lady presented to the urology clinic after an enhanced computed tomography (CT) scan of the abdomen and pelvis was done for abdominal distention and right upper quadrant discomfort of several weeks duration. She denied any flank pain, hematuria, lower urinary tract symptoms, fever, chills, or even lower extremity edema. The patient denied any family history of kidney diseases.

The CT scan reported a predominantly fat-containing mass arising from the medial interpolar region of the right kidney, measuring about 13 cm × 19 cm in size, abutting the inferior border of the liver, gallbladder, duodenum, hepatic flexure of the colon, and the medial aspect of the right psoas muscle. The mass involved the renal vein, with a fat thrombus extending up to the infrahepatic portion of the vena cava, just below the confluence of the hepatic veins (Fig. 1). The tumor within the IVC is partially occlusive. Our differential at this stage was either an aggressive renal AML or a retroperitoneal liposarcoma, given the extent of the disease. Although low in our differential, we also suspected Tuberous Sclerosis, but genetic testing came out negative.

For further characterization of this considerable mass and to accurately identify vital surrounding structures, vessels, and surgical planes for intraoperative planning, we performed an enhanced magnetic resonance imaging (MRI) imaging of the abdomen and pelvis with both arterial and venous phases. A predominately fat-containing renal mass, mostly of the classic type, was again noted, measuring 13 cm × 9.7 cm × 19 cm, with a fat thrombus extending 2.5 cm below the confluence of the hepatic veins. The right renal artery was seen crossing the middle of the lesion. Several thin enhancing septations were seen within the mass, along with an aneurysmal dilatation (Fig. 2).

Given the extension of the mass along with the fear for extension of thrombus and possible embolus, a multidisciplinary decision was made to proceed with a transabdominal exploration of the retroperitoneal mass, through a Mercedes Benz modification of an extended subcostal incision. Intraoperatively and after colonic mobilization, the large fat-predominant mass was seen arising from the right renal hilum and abutting superiorly the liver bed, and laterally deviating the great vessels. A right radical nephrectomy, adrenalectomy, para-caval lymphadenectomy was performed, along with a complete caval thrombectomy, successfully performed after complete liver mobilization, with suprahepatic vena caval and contralateral left renal vein clamping to diminish back bleeding for proper sewing of the venotomy line (Fig. 3). No intraoperative complications were encountered, and blood loss was around 400 cc. The patient was discharged home 6 days later with a smooth postoperative course.

The final histopathology was consistent with a classic AML with no epithelioid features. The mass measured 13 cm × 10 cm × 19cm in size and was arising from the renal hilum. The mass had a homogenous cut surface with few visible blood vessels. The fat thrombus extracted from the venotomy was also consistent with a classical AML (Fig. 4). All excised

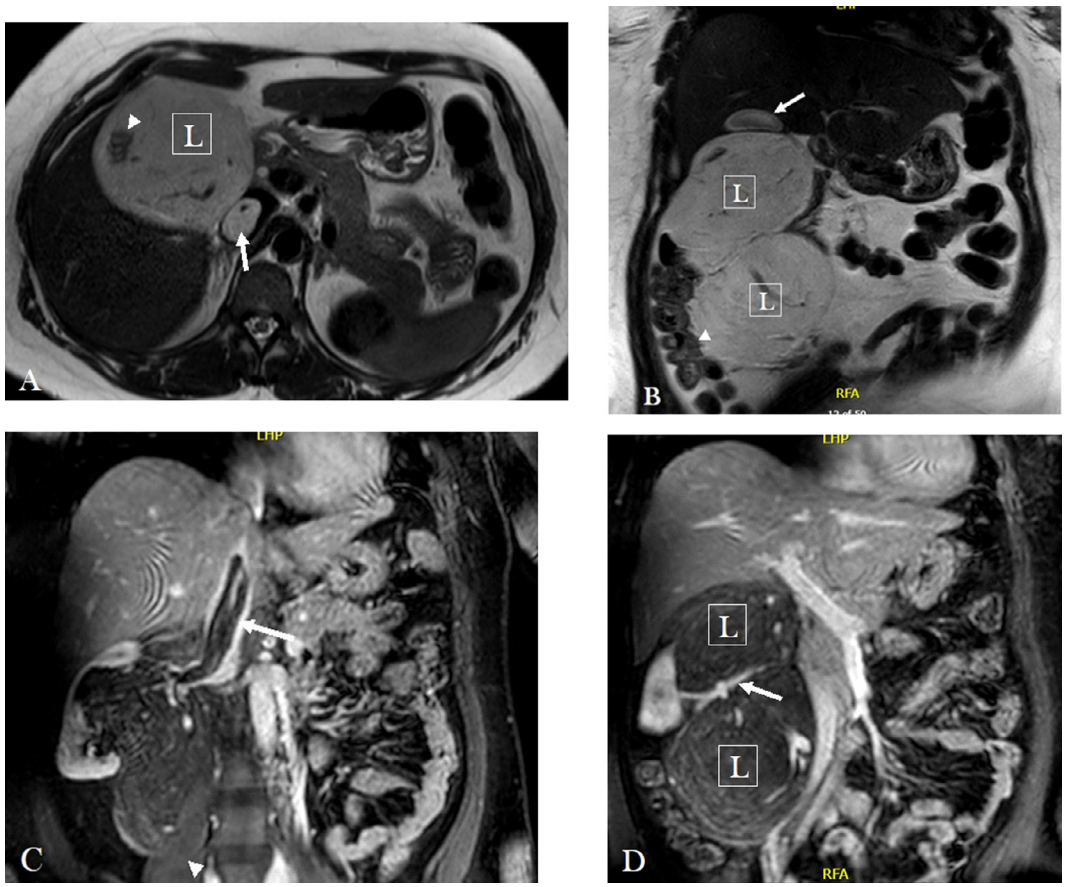

Fig. 2 – (A) Axial cross-section of T2-sequence of MRI revealing the presence of right large fat-containing renal mass (L), consistent with classic AML, along with the presence of a small peripheral aneurysm within the AML (arrowhead), and the presence of fat thrombus within the inferior vena cava (arrow), partially occluding it. (B) Coronal cross-section of the MRI, T2 sequence, showing a large bi-lobed right renal mass (L), measuring 13 x 9.7 x 19 cm, composed almost entirely of fat. The mass is seen extending laterally and cephalad, abutting and deviating the ascending colon (arrowhead) and the gallbladder (arrow), respectively. (C) Another Coronal cross-sectional image of the enhanced MRI during the venous phase, showing the large AML, protruding from the interpolar region and in contact with the right psoas muscle (arrowhead). An intramural fat thrombus is also seen extending cephalad within the IVC, to approximately 2.5 cm below the confluence of the hepatic veins (arrow). (D) Coronal cross-sectional image during venous phase showing a branch of renal artery (arrow) supplying the lower pole of the right kidney. Also noted this same branch of renal artery divides the huge AML into 2 lobes (L).

lymph nodes were benign and not involved with neither malignant nor metastatic cells.

Discussion

Renal AMLs are typically composed of adipose tissues, blood vessels, and smooth vessels [5], and has been characterized as part of the PEComas family (perivascular epithelioid cell differentiation) [6]. PEComas are a group of mesenchymal neoplasms that are strongly associated with tuberous sclerosis and tumor suppressor genes, TSC1 and TSC2 [7].

Renal AML are the most frequently encountered benign renal tumors, originating from renal parenchyma rather than the capsule or perinephric tissue, with an estimated prevalence between 0.2% and 0.6%, and female predilection of 2:1 [8]. Hereditary lesions affect both genders equally and usually manifest at a younger age, and are usually large, bilateral, and tend to be more aggressive [9].

With the increased use of various radiological modalities, more than 80% of renal AMLs are nowadays discovered incidentally, with hemorrhage at clinical presentation seen in 15% of cases, that is, so-called "Wunderlich syndrome." In contrast, others may present with hemorrhagic shock in less than 10% of those cases [10]. Using an ultrasound, classic AMLs are almost always hyperechoic compared to the renal parenchyma due to the presence of macroscopic fat [6]. However, ultrasounds are never accurately and solely used in diagnosing AML but can be used as a follow-up tool instead [11].

Alternatively, CT scans have excellent sensitivity, specificity, positive, and negative predictive values in distinguishing AMLs [6]. The most hypodense area within a classic AML would have an attenuation value of −15 HU or less,

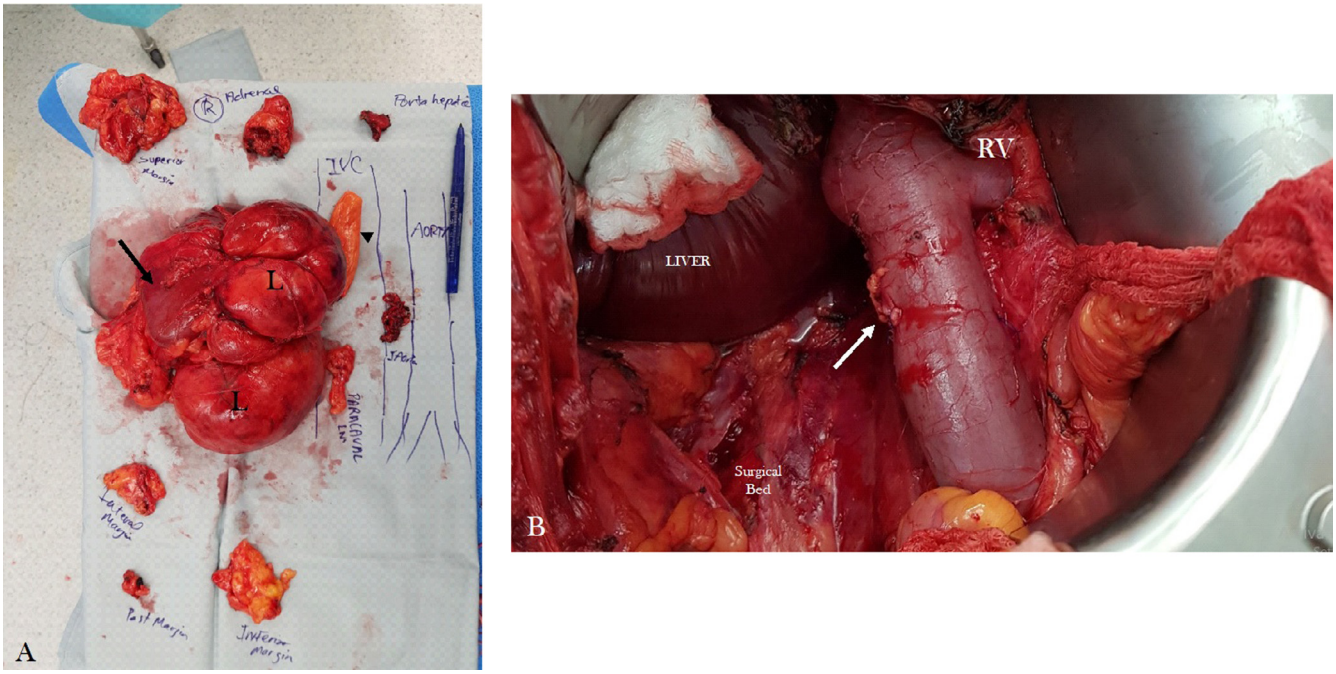

Fig. 3 – (A) Gross resected specimen placed outside the surgical field in the same anatomic orientation. The normal kidney parenchyma is shown (arrow), with the protruding of a bi-lobed angiomyolipoma (L). The fat thrombus within the IVC is also shown (arrowhead). Other tissues shown are right adrenal gland, para-aortic and interaortocaval lymph node, along with multiple surgical margins taken. (B) Image showing specimen after removal, with the IVC venotomy suture line (arrow) and surgical bed. The liver and left renal vein (RV) is shown too.

suggestive of a macroscopic fat content. Nevertheless, in a small portion of AMLs, around 4%-5%, intralesional fat cannot be detected due to its minute amount in these rare lesions, the so-called fat-poor or fat-invisible renal AMLs. Those lesions, in particular, represent a diagnostic challenge to both radiographers and urologists, as they closely mimic renal cell carcinomas (RCC) [12]. Renal AMLs rarely contain calcifications, a diagnostic finding that could differentiate it from RCCs [13]. Unenhanced CT scans will not differentiate fat-poor from fat-invisible AMLs, and as such, a chemical shift imaging (CSI) technique using MRI would be better utilized [14].

MRI is another tool that is equivalent to CT in diagnosing AMLs, and even more potent in diagnosing fat-poor AMLs [12]. An unenhanced MRI is just needed to diagnose AML, which is of particular significance in patients with compromised renal function [6]. Comparing T1-weighted images with and without frequency, selective fat suppression allows for the detection of macroscopic fat within an AML lesion. Renal masses that are hyperintense before fat suppression and hypointense after frequency selective fat suppression are usually consistent with AML [15]. Another MRI sequence, useful in differentiating fat-poor AML from RCC especially that typical T1 sequence findings may not be straightforward, is in phase vs opposed phase chemical shift sequencing. CSI results in a sharp black boundary, the so-called "India-ink artifact" at the interface of macroscopic fat, found in AMLs, and water, contained in the renal parenchyma [15]. On CSI-MRI, a fat-poor AML would exhibit a tumor-to-spleen ratio less than 0.71 or a signal intensity index of more than 16.5%. On the contrary, the too little fat seen in fat-invisible AMLs would exhibit a tumor-to-spleen ratio ratio of more than 0.71 and a signal intensity index less than 16.5% [14].

The role and data on positron emission tomography scans utilizing fluorine-18 fluoro-2-deoxy-D-glucose for differentiating renal AMLs vs other forms of RCCs, is still scarce and controversial. The true positive rate for detecting RCC using positron emission tomography/CT fluorine-18 fluoro-2-deoxy-D-GLUCOSE scan is around 77%, and that for detecting recurrent or metastatic RCC is around 85% [16]. RCC lesions generally exhibit a much higher SUVmax, than AMLs [17].

Histologically, renal AMLs are broadly classified as typical or atypical AMLs. The former classification is otherwise referred to as triphasic or classic type, where all 3 components are present in the lesion. The detection of adipose tissue on imaging is a crucial criterion for any classic AML, as previously highlighted [6]. On the contrary, atypical AMLs are referred to as monophasic, that is, consisting almost exclusively of one component while other elements are present in very small portions, or the epithelioid variant, consisting of numerous epithelioid muscle cells with abundant eosinophilic and granular cytoplasm and few if no fat cells [5]. Risk factors for malignant AML include size greater than 7 cm, tumor necrosis, and epitheliod carcinoma-like pattern [18].

Grossly, renal AMLs are generally well circumscribed with a tan-white to yellow cut surface, depending on the lipid content. Hemorrhage can be seen, but necrosis is rare. Adipocytes are usually intermingled with the spindle cells and are mature without any cytologic atypia [6].

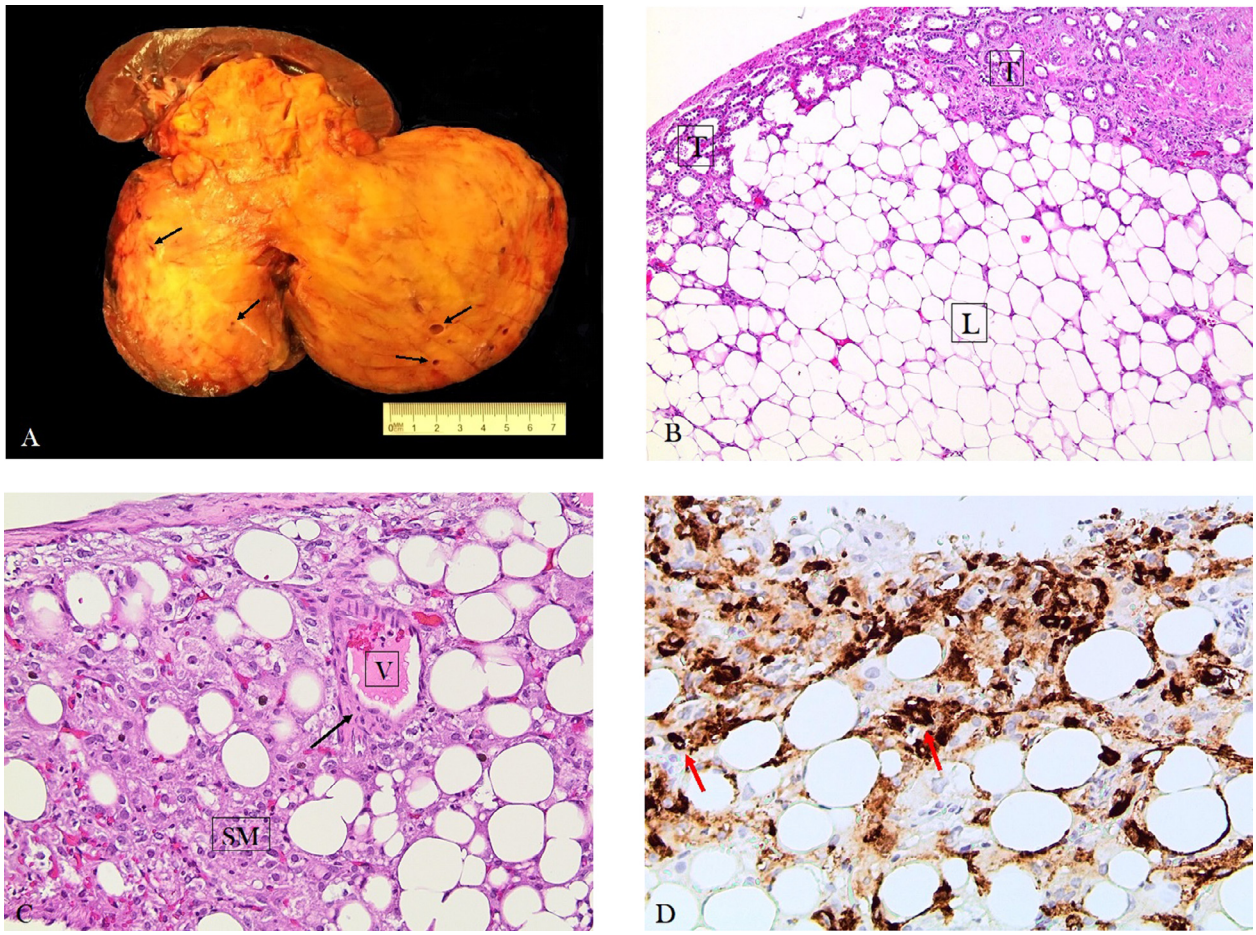

Fig. 4 – (A) A large lobulated angiomyolipoma protruding from the hilum of the kidney. Its cut surface is predominantly fatty and shows few grossly visible vascular channels (arrows). (B) Predominantly lipomatous portion of the tumor (L) interfacing with normal renal tubules (T). Hematoxylin and eosin, 100×. (C) A rare area of increased tumor cellularity composed of sheets of rounded smooth muscle cells (SM) between mature fat cells. A tumor blood vessel (arrow, V) is also noted in this picture. Hematoxylin and eosin, ×400. (D) Positive immunostaining of myoid tumor cells for HMB-45 (arrows) (×400).

There have been infrequently reported cases of AML, especially of the classic type, that has extended into the IVC. The current thinking behind this extension is based on multifocal tumorigenesis, rather than metastasis [19]. To our knowledge, 65 cases have been reported so far for classic renal AMLs with vascular extension, either to the renal vein, IVC, or even cephalad toward the right atrium (Table 1). Analysis of those cases reveals the following: a female predilection, 79% (52/66) were right-sided kidney tumors, and most patients (around 62%) had presenting symptoms, mainly flank or abdominal pain.

It has been postulated that surgical treatment is required, whenever renal AML extend into great vessels, even if they are asymptomatic, due to the risk of fatal embolism to the heart or pulmonary veins [20]. Multiple attempts at minimally invasive approaches have been attempted, including selective arterial embolization (SAE) with or without radiofrequency ablation, and have been relatively effective [21]; yet, surgical excision has been the most durable and oncologically safe approach.

Indeed, before any surgical planning, a proper diagnosis of AML is a must. Most AMLs can be diagnosed by imaging, as stated above. In case of difficulty, especially for fat-poor or fat-invisible AMLs vs small-sized RCCs and inconclusive imaging, whether CT and/or MRI, a percutaneous biopsy is recommended in this situation [22].

The optimal surgical treatment would be a nephron-sparing surgery (NSS), since the disease is primarily benign, and this would yield superior renal functional outcomes, and carries a lower mortality compared to radical nephrectomy. These conclusions mimic those extrapolated from series on partial nephrectomy cases for RCC [23]. Given that renal AMLs with extension to renal vessels and IVC tend to be huge compared to isolated lesions within the kidney, and in proximity to major organs and/or vessels, nephrectomy is a safer operative decision, such as the case presented above. Caval thrombectomy follows similar surgical principles as that for RCC and careful dissection of preoperative images is imperative, for the optimal planning of cross clamping of the vena cava.

The literature highlights several options for the management of renal AMLs in general. Initially, advocates for interventions are those for symptomatic lesions larger than

Table 1 – List of all renal classic angiomyolipoma cases with extra-renal/vascular extension.

Case	Authors, year	Age/sex	Laterality	Tumor size	Thrombus level	Therapy
1	Kutcher et al, 1982	16/F	Right	Large	IVC	Nephrectomy
2	Brantly et al, 1985	45/F	Right	9cm	IVC	Nephrectomy
3	Rothenberg et al, 1986	62/F	Left	4.5 cm	Right atrium	Nephrectomy
4	Camunez et al, 1987	22/F	Right	Small	IVC	Follow-up
5	Arenson et al, 1988	22/F	Right	8.5 cm	IVC	Nephrectomy
6	Byrne et al, 1988	56/F	Right	13.5 cm	IVC	Nephrectomy
7	Umeyama et al, 1992	75/F	Bilateral	16 cm	IVC and renal vein	Partial nephrectomy
8	Reiff et al, 1993	58/F	Right	10 cm	IVC	Nephrectomy
9	Honda et al, 1993	58/F	Right	Not mentioned	IVC	Nephrectomy
10	Moulin et al, 1994	36/F	Right	Large	IVC	Nephrectomy
11	Matsuura et al, 1995	34/F	Right	Large	IVC	Nephrectomy
12	Baert et al, 1995	53/F	Right	6.5 cm	IVC	Nephrectomy
13	Hibi et al, 1995	31/F	Right	10 cm	IVC	Nephrectomy
14	Leder et al, 1995	30/F	Right	Not mentioned	IVC	Nephrectomy
15	Briones et al, 1996	64/M	Right	6.5 cm	IVC	Nephrectomy
16	Citadini et al, 1996	65/F	Left	6 cm	IVC	Follow-up
17	Citadini et al, 1996	67/M	Right	6 cm	IVC	Nephrectomy
18	Citadini et al, 1996	54/F	Right	4 cm	Renal vein	Follow-up
19	Citadini et al, 1996	19/F	Left	8 cm	Renal vein	Nephrectomy
20	Rubio-Briones et al, 1997	64/M	Right	6.5 × 4 cm	IVC	Nephrectomy, cavotomy
21	Bernstein et al, 1997	45/M	Right	6 × 11 cm	IVC	Pre-op kidney embolization, nephrectomy, thrombus extraction
22	Martignoni et al, 1998	60/M	Left	6 cm	IVC	Nephrectomy
23	Gotoh et al, 1998	52/F	Right	3.5 cm	IVC	Nephrectomy
24	Christiano et al, 1999	42/M	Right	20.5 cm	IVC	Nephrectomy
25	Ito et al, 1999	40/F	Right	Not mentioned	Right atrium	Nephrectomy, thrombectomy using extracorporeal circulation
26	Toda et al, 1999	41/F	Right	18-cm tumor 13-cm thrombus	IVC + right atrium	Nephrectomy
27	Davydov et al, 2001	46/F	Right	6 cm	IVC and right atrium	Nephrectomy
28	Kawaguchi et al, 2002	40/F	Bilateral	20 cm	IVC	Died during nephrectomy
29	Shangra et al, 2002	69/F	Right	10 cm	IVC	Nephrectomy
30	Wilson et al, 2002	69/F	Right	10 cm	IVC	Nephrectomy
31	Hatakeyama et al, 2002	31/F	Right	11 cm	IVC	Nephrectomy
32	Islam et al, 2003	40/F	Right	11 cm	IVC	Nephrectomy
33	Chandrasoma et al, 2004	61/M	Left	4 cm	IVC	Partial nephrectomy
34	Chandrasoma et al, 2004	20/M	Right	17.5 cm	IVC	Nephrectomy
35	Islam et al, 2004	40/F	Right	11 cm	IVC	Nephrectomy
36	Bibier et al, 2005	36/M	Right	Not mentioned	IVC	Nephrectomy
37	Haritharan et al, 2006	48/F	Right	15 cm	IVC	Nephrectomy
38	Park et al, 2007	69/M	Bilateral	13 cm	IVC	Nephrectomy
39	Ban et al, 2008	70/F	Right	14 cm	IVC	Nephrectomy
40	Shigeo Takebayashi et al, 2008	47/F	Left	7 cm	Renal vein	Nephrectomy
41	Quicios Dorado et al, 2008	41/F	Left	Not mentioned	IVC and right atrium	Nephrectomy
42	Dinis da Gama et al, 2008	39/F	Right	Not mentioned	IVC	Nephrectomy
43	Sandstrom et al, 2009	31/M	Left	6 cm	IVC with fat embolus in Rt Pulm. artery	Nephrectomy + embolectomy
44	Luo et al, 2010	27/F	Right	4 cm	IVC	Nephrectomy
45	Tan YS et al, 2010	44/M	Right	9.7 × 6.6 × 14.7 cm	IVC	Nephrectomy + IVC; venous clamp 12 min
46	Jonathan Lopater et al, 2011	34/F	Right	4 cm	IVC	Nephrectomy
47	Mittal et al, 2011	46/F	Right	7 cm	IVC	Nephrectomy
48	Luo et al, 2011	27/F	Right	4 cm	IVC	Nephrectomy
49	Bakshi et al, 2011	40/F	Right	Not mentioned	IVC	Nephrectomy + Thrombectomy
50	Li H et al, 2012	43/F	Right	5.5 × 4.0 × 4.2 cm	IVC	Nephrectomy + venous thrombectomy
51	Xiaoman Li et al, 2013	52/F	Right	12.5 cm	IVC and right atrium	Nephrectomy

(*continued on next page*)

Table 1 (*continued*)

Case	Authors, year	Age/sex	Laterality	Tumor size	Thrombus level	Therapy
52	Campbell Grant et al, 2013	22/F	Right	9 cm	IVC	Nephrectomy
53	Yarmish et al, 2013	70/F	Left	Not mentioned	Renal vein + bilateral pulmonary arteries fat thrombus	Nephrectomy
54	Fernandez-Pello et al, 2013	22/F	Right	8 cm	IVC	Lap. Nephrectomy + thrombectomy
55	Xin-xiang Que et al, 2013	41/M	Right	8 cm	IVC	Nephrectomy
56	Harris et al, 2014	70/F	Left	12 cm	Renal vein + fat embolism in Rt pulmonary artery	Nephrectomy
57	Shen et al, 2014	77/F	Right	Not mentioned	IVC	Open radical nephrectomy + IVC thrombectomy
58	Hamidi et al, 2015	43/F	Right	5 cm	IVC with Rt pulm art fat thrombus	Nephrectomy
59	Celik et al, 2015	33/F	Right	5.6 × 4.0 cm	IVC; fat thrombus to left pulmonary artery	Nephrectomy with tumor thrombectomy
60	Veedu Prasad et al, 2016	50/F	Left	12 cm	Right atrium	Nephrectomy
61	Chen Y-H et al, 2016	37/M	Right	5.1 × 4.4 cm	IVC	Lap. Nephrectomy; workbench partial nephrectomy followed by auto-transplant
62	Majdoub et al, 2017	37/?	Right	6.2 × 7.8 cm	Renal vein	Nephrectomy
63	Cornman-Homonoff et al, 2017	43/F	Right	10.1 × 8.9 × 14.8 cm	IVC	Pre-op embolization; IVC filter; radical nephrectomy with tumor thrombectomy
64	Gu et al, 2018	41/M	Right	7.5 × 6.0 cm	IVC + pulmonary arteries	Radical nephrectomy + CABG for thrombus removal
65	Galiabovitch et al, 2019	70/F	Right	4.8 cm	Renal vein	Laparoscopic nephrectomy
66	Present Case, 2019	40/F	Right	13 × 9.7 × 19 cm	IVC	Nephrectomy

IVC, inferior vena cava.

4 cm, lesions with suspected malignancy, and lesions found in women with childbearing age [24]. Other indications would be the presence of aneurysms larger than 5 mm [25], concomitant Tuberous sclerosis complex (TSC) syndrome, as lesions in this situation tend to have faster growth rate (1.25 cm vs 0.19 cm yearly for sporadic AMLs) [26], and poor access to emergency care as considerations to proceed with intervention in case of bleeding. The absence of these indications mandates that active surveillance is a valid option [6]. Unfortunately, no current prospective randomized clinical trials have compared active surveillance vs treatment for AMLs and no strict criteria on the frequency of follow-up of such cases.

Partial nephrectomy for renal AMLs has been reported in few case series, the largest being reported by Boorjian et al in 2007, including 58 patients who underwent open NSS for sporadic AML, having a mean size of 3.9 cm (0.8-12.5 cm). Seven (12%) complications were noted, with 2 (3.4%) recurrence rate in this series, with a mean follow-up of 8 years [27].

For patients in whom NSS is not feasible due to size, extension to vessels, and tumor location, another alternative would be to proceed to radical nephrectomy or SAE. The latter is an attractive option in case of acute hemorrhage and hemodynamic instability [6]. Numerous agents have been used for embolization with no superiority of one agent over another [6]. The recurrence rate post-SAE is highly variable and ranges between 11% and 40% [28].

Percutaneous ablation is also another minimal invasive modality but restricted to small AMLs and asymptomatic lesions. Unfortunately, no long-term data are available for this modality [29].

Finally, mammalian Target of Rapamycin pathway inhibitors such as Sirolimus or Everolimus, aims to halt tumor progression and regression of size in existing tumors in hereditary AML and LAM syndrome. Several phase II trials using Sirolimus for AML included a total of 94 patients with a 46.8% response rate after 12 months, but no complete response was shown [30].

Conclusion

Renal AML of classic subtype remains to be a benign entity, although few cases of its outspread to renal vessels and beyond are reported. Proper use of various imaging modalities is crucial to obtain adequate diagnosis and to base our future management on. Optimal treatment options are still not well defined and versatile. Surgery seems to be inevitable in cases similar to ours, with extension to IVC, for fear of embolus. Sur-

geons performing such complex procedures must be trained to do so, especially that complete liver mobilization may be necessary for proper venotomy and thrombectomy.

Acknowledgment

The authors thank Dr Ayman Tawil, Professor of clinical specialty from the Department of Pathology and Laboratory Medicine, for providing the gross and the histopathologic images with their valuable description.

Authors' contributions

Degheili JA and Abou Heidar NF carried out the literature review and wrote the manuscript, including the case presentation. Abi Saad G and Khauli R performed proofreading of the manuscript. Abou Heidar NF and Degheili JA contributed mostly in obtaining the radiological images. All authors have agreed on the final version of the manuscript, prior to submission.

Informed consent

A written informed consent was obtained from the patient himself for the publication of this case report, along with all corresponding figures. A copy of the written consent is available for review by the Editor-in-Chief of this journal, upon his request.

REFERENCES

[1] Bharwani N, Christmas TJ, Jameson C, Moat N, Sohaib SA. Epithelioid angiomyolipoma: imaging appearances. Br J Radiol 2009;82(984):e249–52 PMID:19934066 .
[2] Oesterling JE, Fishman EK, Goldman SM, Marshall FF. The management of renal angiomyolipoma. J Urol 1986;135(6):1121–4 PMID:.
[3] Aydin H, Magi-Galluzzi C, Lane BR, Sercia L, Lopez JI, Rini BI, et al. Renal angiomyolipoma: clinicopathologic study of 194 cases with emphasis on the epithelioid histology and tuberous sclerosis association. Am J Surg Pathol 2009;33(2):289–97 PMID:.
[4] Tan YS, Yip KH, Tan PH, Cheng WS. A right renal angiomyolipoma with IVC thrombus and pulmonary embolism. Int Urol Nephrol 2010;42(2):305–8 PMID:19609707 .
[5] Vos N, Oyen R. Renal Angiomyolipoma: the Good, the Bad, and the Ugly. J Belg Soc Radiol 2018;102(1):41 PMID:30039053 .
[6] Flum AS, Hamoui N, Said MA, Yang XJ, Casalino DD, McGuire BB, et al. Update on the diagnosis and management of renal angiomyolipoma. J Urol 2016;195(4 Pt 1):834–46 PMID:26612197 .
[7] Montironi R, Cheng L, Scarpelli M, Lopez-Beltran A. Pathology and genetics: tumours of the urinary system and male genital system: clinical implications of the 4th edition of the WHO classification and beyond. Eur Urol 2016;70(1):120–3 PMID:26996660 .
[8] Fittschen A, Wendlik I, Oeztuerk S, Kratzer W, Akinli AS, Haenle MM, et al. Prevalence of sporadic renal angiomyolipoma: a retrospective analysis of 61,389 in- and out-patients. Abdom Imaging 2014;39(5):1009–13 PMID:24705668 .
[9] Lane BR, Aydin H, Danforth TL, Zhou M, Remer EM, Novick AC, et al. Clinical correlates of renal angiomyolipoma subtypes in 209 patients: classic, fat poor, tuberous sclerosis associated and epithelioid. J Urol 2008;180(3):836–43 PMID:18635231 .
[10] Sooriakumaran P, Gibbs P, Coughlin G, Attard V, Elmslie F, Kingswood C, et al. Angiomyolipomata: challenges, solutions, and future prospects based on over 100 cases treated. BJU Int 2010;105(1):101–6 PMID:19493268 .
[11] Steiner MS, Goldman SM, Fishman EK, Marshall FF. The natural history of renal angiomyolipoma. J Urol 1993;150(6):1782–6 PMID:8230504 .
[12] Kim JK, Kim SH, Jang YJ, Ahn H, Kim CS, Park H, et al. Renal angiomyolipoma with minimal fat: differentiation from other neoplasms at double-echo chemical shift FLASH MR imaging. Radiology 2006;239(1):174–80 PMID:16507752 .
[13] Hammadeh MY. Calcification within angiomyolipoma. Radiographics 1998;18(1):4 Jan-FebPMID:9460105 .
[14] Park BK. Renal angiomyolipoma: radiologic classification and imaging features according to the amount of fat. AJR Am J Roentgenol 2017;209(4):826–35 PMID:28726505 .
[15] Jinzaki M, Silverman SG, Akita H, Nagashima Y, Mikami S, Oya M. Renal angiomyolipoma: a radiological classification and update on recent developments in diagnosis and management. Abdom Imaging 2014;39(3):588–604 PMID:24504542 .
[16] Martínez de Llano SR, Delgado-Bolton RC, Jiménez-Vicioso A, Pérez-Castejón MJ, Carreras Delgado JL, et al. [Meta-analysis of the diagnostic performance of 18F-FDG PET in renal cell carcinoma]. Rev Esp Med Nucl 2007;26(1):19–29 Jan-FebPMID:17286945 .
[17] Namura K, Minamimoto R, Yao M, Makiyama K, Murakami T, Sano F, et al. Impact of maximum standardized uptake value (SUVmax) evaluated by 18-Fluoro-2-deoxy-D-glucose positron emission tomography/computed tomography (18F-FDG-PET/CT) on survival for patients with advanced renal cell carcinoma: a preliminary report. BMC Cancer 2010;10:667 PMID:21129184 .
[18] Christiano AP, Yang X, Gerber GS. Malignant transformation of renal angiomyolipoma. J Urol 1999;161(6):1900–1 PMID:10332463 .
[19] Lin WY, Chuang CK, Ng KF, Liao SK. Renal angiomyolipoma with lymph node involvement: a case report and literature review. Chang Gung Med J 2003;26(8):607–10 PMID:14609043 .
[20] Shen G, Mao Q, Yang H, Wang C. Aggressive renal angiomyolipoma with vena cava extension: a case report and literature review. Oncol Lett 2014;8(5):1980–2 PMID:25295081 .
[21] Stamatiou KN, Moschouris H, Marmaridou K, Kiltenis M, Kladis-Kalentzis K, Malagari K. Combination of superselective arterial embolization and radiofrequency ablation for the treatment of a giant renal angiomyolipoma complicated with caval thrombus. Case Rep Oncol Med 2016;2016:8087232 PMID:27293932 .
[22] Sahni VA, Silverman SG. Biopsy of renal masses: when and why. Cancer Imaging 2009;9:44–55 Jul 6PMID:19602467 .
[23] Thompson RH, Boorjian SA, Lohse CM, Leibovich BC, Kwon ED, Cheville JC, et al. Radical nephrectomy for pT1a renal masses may be associated with decreased overall survival compared with partial nephrectomy. J Urol 2008;179(2):468–71 discussion 472-3PMID:18076931 .
[24] Preece P, Mees B, Norris B, Christie M, Wagner T, Dundee P. Surgical management of haemorrhaging renal angiomyolipoma in pregnancy. Int J Surg Case Rep 2015;7C:89–92 PMID:25598402 .

[25] Yamakado K, Tanaka N, Nakagawa T, Kobayashi S, Yanagawa M, Takeda K. Renal angiomyolipoma: relationships between tumor size, aneurysm formation, and rupture. Radiology 2002;225(1):78–82 PMID:12354988 .
[26] Seyam RM, Bissada NK, Kattan SA, Mokhtar AA, Aslam M, Fahmy WE, et al. Changing trends in presentation, diagnosis and management of renal angiomyolipoma: comparison of sporadic and tuberous sclerosis complex-associated forms. Urology 2008;72(5):1077–82 PMID:18805573 .
[27] Boorjian SA, Frank I, Inman B, Lohse CM, Cheville JC, Leibovich BC, et al. The role of partial nephrectomy for the management of sporadic renal angiomyolipoma. Urology 2007;70(6):1064–8 PMID:18158015 .
[28] Chick CM, Tan BS, Cheng C, Taneja M, Lo R, Tan YH, et al. Long-term follow-up of the treatment of renal angiomyolipomas after selective arterial embolization with alcohol. BJU Int 2010;105(3):390–4 PMID:.
[29] Tan YK, Best SL, Olweny E, Park S, Trimmer C, Cadeddu JA. Radiofrequency ablation of incidental benign small renal mass: outcomes and follow-up protocol. Urology 2012;79(4):827–30 PMID:22309782 .
[30] Peng ZF, Yang L, Wang TT, Han P, Liu ZH, Wei Q. Efficacy and safety of sirolimus for renal angiomyolipoma in patients with tuberous sclerosis complex or sporadic lymphangioleiomyomatosis: a systematic review. J Urol 2014;192(5):1424–30 PMID:24813310 .